Engineering xxx (xxxx) xxx

Contents lists available at ScienceDirect

Engineering

journal homepage: www.elsevier.com/locate/eng

Research
Tunnel Engineering—Article

Rockburst Hazard Control Using the Excavation Compensation Method (ECM): A Case Study in the Qinling Water Conveyance Tunnel

Jie Hu [a,b], Manchao He [a,b], Hongru Li [a,*], Zhigang Tao [b], Dongqiao Liu [b], Tai Cheng [a], Di Peng [b]

[a] Department of Geotechnical Engineering, College of Civil Engineering, Tongji University, Shanghai 200092, China
[b] State Key Laboratory for Geomechanics and Deep Underground Engineering, China University of Mining and Technology, Beijing 100083, China

ARTICLE INFO

Article history:
Available online xxxx

Keywords:
Rockburst
Excavation compensation method
Pre-stressed support
Negative Poisson's ratio bolt
Tunnel boring machine

ABSTRACT

Rockburst disasters occur frequently during deep underground excavation, yet traditional concepts and methods can hardly meet the requirements for support under high geo-stress conditions. Consequently, rockburst control remains challenging in the engineering field. In this study, the mechanism of excavation-induced rockburst was briefly described, and it was proposed to apply the excavation compensation method (ECM) to rockburst control. Moreover, a field test was carried out on the Qinling water conveyance tunnel. The following beneficial findings were obtained: Excavation leads to changes in the engineering stress state of surrounding rock and results in the generation of excess energy ΔE, which is the fundamental cause of rockburst. The ECM, which aims to offset the deep excavation effect and lower the risk of rockburst, is an active support strategy based on high pre-stress compensation. The new negative Poisson's ratio (NPR) bolt developed has the mechanical characteristics of high strength, high toughness, and impact resistance, serving as the material basis for the ECM. The field test results reveal that the ECM and the NPR bolt succeed in controlling rockburst disasters effectively. The research results are expected to provide guidance for rockburst support in deep underground projects such as Sichuan–Xizang Railway.

1. Introduction

Rockburst disasters occur frequently in underground rock engineering with high geo-stress, causing both casualties and damage to mechanical equipment. It seriously affects the safety of construction, especially as the underground engineering is gradually entering deep strata in China [1]. At present, a growing number of mines and tunnels are developed into the depth of more than 1000 m underground and faced with serious rockburst risk. For example, on November 28, 2009, a strong rockburst accident occurred in the super deep Jinping Ⅱ Hydropower Station in China (maximum buried depth over 2500 m), resulting in seven deaths, one injury, and the destruction of a tunnel boring machine (TBM) [2]. The maximum buried depth and geo-stress of the tunnel in the Ya'an–Linzhi section of Sichuan–Xizang Railway under construction are 2080 m and 53.06 MPa, respectively, and 27 tunnels there are likely to encounter rockburst [3].

In recent decades, numerous researches concerning rockburst have been reported, including those on its definition, classification, failure mechanism, risk assessment, and early warning. It is generally believed that rockburst is a kind of unconventional and dynamic failure caused by the violent release of strain energy and accompanied with the ejection of rock fragments and the generation of huge sounds [1,4–8]. It is closely related to lithology and structural characteristics of surrounding rock, engineering geological conditions, excavation technology, and so forth [9–12]. According to different inducing mechanisms, rockburst can be roughly divided into two categories [13]: One is strainburst caused by radial stress unloading and tangential stress concentration during excavation, and the other is impact-induced rockburst caused by dynamic disturbance (fault slip, earthquake, and blasting, etc.) of surrounding rock under static stress after excavation. Considering that the former is more common in engineering practice, it is taken as the main research object in this study. A large number of laboratory tests, such as static uniaxial (or biaxial) compression tests [14–16] and dynamic tests based on the split Hopkinson bar [17,18], have been carried out to reveal the mechanism of rockburst kinetic energy. He et al. [19] put forward the test method

* Corresponding author.
E-mail address: lihongru@tongji.edu.cn (H. Li).

https://doi.org/10.1016/j.eng.2023.11.013

of true triaxial loading and single-side unloading, developed a set of true triaxial strainburst experimental machine, and successfully realized the simulation of excavation-induced strainburst in the laboratory, which provided a basis for revealing the mechanism of rockburst. In addition, a rigid experimental machine simulating impact-induced rockburst by superimposing dynamic and static loads was also developed [13]. Comprehensive index evaluation methods that take into account factors such as lithology, stress state, and geological conditions in rockburst risk evaluation are considered to have more considerable application prospects [20,21]. Geophysical methods such as acoustic emission (microseismic) [22–25,48], electromagnetic radiation [26], infrared radiation [27], and seismic velocity tomography [28] have also provided reference indicators. In addition, the prediction method combined with artificial intelligence is attracting wide attention [20,29,30].

In the aspect of rockburst control, active pretreatment methods have been adopted for rockburst risk reduction, including optimized excavation scheme [22], destress blasting [31], drilling pressure relief [32], hydraulic fracturing [33], and so forth. The purpose is to avoid partial stress concentration and energy accumulation. The anchorage support system including bolt and cable is still the most commonly used means to control the stability of surrounding rock. However, traditional bolts often undergo brittle breakage and failure under the high geo-stress, failing to provide effective support. With the accumulation of experience, rockburst support strategies gradually change from high-strength support to energy-absorbing support [34,35], which requires that the bolt has not only high strength but also the ability to bear severe deformation. Energy-absorbing support is superior in its capability of absorbing the energy generated in the process of rock dynamic failure and alleviating the harm of rockburst. Some energy-absorbing bolts have been developed and applied to the engineering field, such as Roofex bolt [36], Garford bolt [37], D-bolt [38], and Yield-Lok bolt [39]. Despite extensive efforts, rockburst support remains notably challenging in the engineering field, due to the huge contradiction between traditional support concepts and methods and the requirements for deep underground support.

In this paper, first, the phenomenon and mechanism of excavation-induced rockburst were briefly described with the aid of a self-developed true triaxial strainburst experimental machine. Besides, the excavation compensation method (ECM) applicable to high geo-stress deep underground was summarized, which is different from the surrounding rock control concept of shallow and middle strata. Furthermore, a new type of steel-based bolt, called negative Poisson's ratio (NPR) bolt, was taken as the material foundation of the ECM, and its dynamic and static mechanical properties were tested. On this basis, it was proposed to apply the ECM to rockburst control, and the field test was carried out in the Qinling water conveyance tunnel of Hanjiang-to-Weihe River diversion project. The research results are expected to provide guidance for rockburst control in deep underground projects like Sichuan–Xizang Railway.

2. Principle of the ECM in controlling rockburst

2.1. Rockburst mechanism and experimental verification

After deep rock mass excavation, the radial stress of the surrounding rock near the free surface is reduced to zero immediately, and the tangential stress becomes concentrated gradually. The three-dimensional (3D) stress state of the surrounding rock becomes approximately two-dimensional, as depicted in Fig. 1(a). Under high initial geo-stress, as rock unloads, the maximum principal stress σ_{1c} of rock far exceeds the rock strength σ_c without lateral confinement, resulting in instantaneous rockburst. The simplified stress path is marked by the blue line in Fig. 1(b). Under low initial geo-stress, unloading does not cause rock failure. Instead, rockburst occurs in the process of stress adjustment and concentration, which corresponds to a delayed rockburst in engineering. The simplified stress path is marked by the yellow line in Fig. 1(b). The energy stored in the 3D stress state is larger than that required for static failure in the uniaxial (or biaxial) stress state. This part of excess energy ΔE will mainly be converted into rockburst kinetic energy, as illustrated in Fig. 1(c). Therefore, He et al. [13] put forward $\Delta E > 0$ as the rockburst criterion. This criterion regards rockburst as a kind of engineering failure and considers that the kinetic energy release during rockburst differs from the brittle rupture under conventional uniaxial (or biaxial) load conditions. It emphasizes the excavation-induced change in the stress state. Therefore, the key to controlling the risk of rockburst is to avoid excess energy ΔE.

Strainburst experiments under the above two loading paths were carried out. The self-developed triaxial strainburst experimental machine can realize transient unloading on one side and form a free surface through special mechanical structure, which effectively simulates the excavation in engineering practice. For details of this machine, please refer to He et al. [19]. The sample was made of granite with a density of 2.63 g·cm^{-3} and a size of 150 mm × 60 mm × 30 mm. During the experiment, firstly, the rock sample was restored to the preset initial 3D geo-stress state at a low loading rate and maintained the state for 1000 s. Subsequently, the minimum principal stress σ_3 was suddenly unloaded, and the loading of the maximum principal stress σ_1 started by stages to simulate the process of gradual stress concentration after unloading. Fig. 2 presents the instantaneous rockburst of a typical sample. The initial stresses were: σ_1 = 90 MPa, σ_2 = 60 MPa, and σ_3 = 20 MPa. At the moment of unloading, numerous rock fragments were ejected, showing the characteristics of obvious dynamic failure. Fig. 3 illustrates the delayed rockburst of a typical sample. The initial geo-stresses were: σ_1 = 80 MPa, σ_2 = 60 MPa, and σ_3 = 20 MPa. In the stress adjustment stage after unloading, the sample underwent progressive failure. At 4029.245 s of the force holding stage, some rock fragments spalled off. Then, after a quiet period, a full rockburst occurred. The delay process may be attributed to the viscosity of rock.

Recently, the authors' team has developed a new 5000 kN true triaxial rockburst experimental system [40] in the State Key Laboratory for Geomechanics and Deep Underground Engineering (Beijing, China). Developed on the basis of the first-generation strainburst experimental machine and impact-induced rockburst experimental machine, it can realize rapid unloading on multiple sides and apply dynamic disturbance load in different directions. It can support laboratory simulation of various types of strainburst and impact-induced rockburst at different positions, providing powerful conditions for further exploring the mechanism of rockburst in the future.

2.2. Principle of the ECM

In the past long-term practice, the Platts pressure arch theory (PPAT) [41] and the new Austrian tunnelling method (NATM) [42] have been guiding underground tunnel construction. The PPAT holds that rock and soil can be self-stabilized. Specifically, a pressure arch (natural balance arch) will be formed in the upper part of roadway after excavation, and the supporting structure only needs to bear the gravity of rock and soil under the pressure arch. It is a support scheme without stress compensation, which is only suitable for controlling shallow loose rock and soil. The NATM emphasizes making full use of the self-bearing capacity of the surrounding rock and the spatial constraint of the excavation face. It takes bolt and shotcrete as the main supporting means and

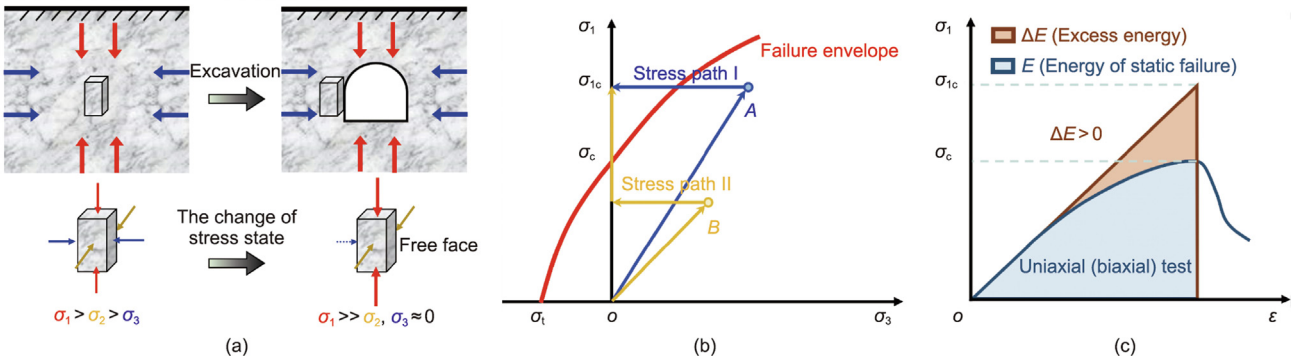

Fig. 1. Mechanism of strainburst. (a) Excavation-induced change in the stress state; (b) stress paths of strainburst; (c) $\Delta E > 0$ as rockburst criterion by comparing triaxial stress–strain curves with uniaxial (biaxial) stress–strain curves. [13] σ_1: the maximum principal stress; σ_2: the intermediate principal stress; σ_3: the minimum principal stress; σ_{1c}: the rock strength when rockburst; σ_c: the uniaxial or biaxial compressive strength; σ_t: the tensile strength; ε: the strain.

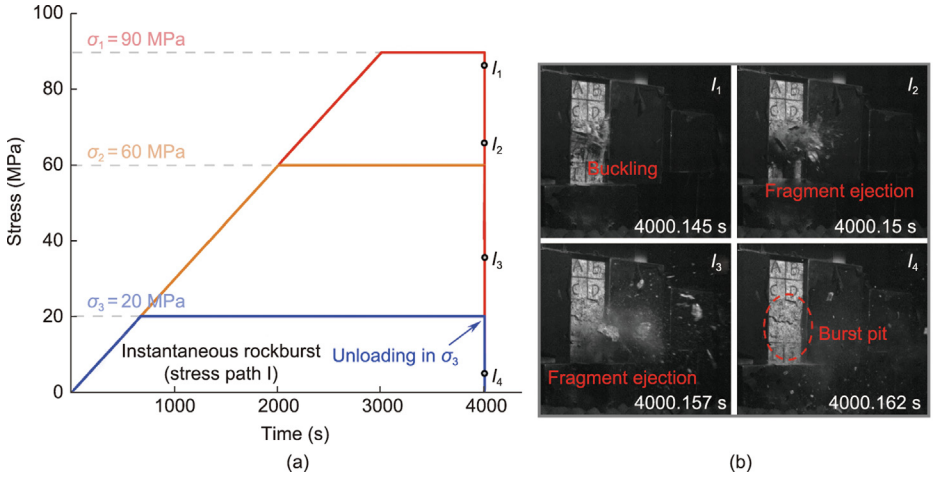

Fig. 2. Instantaneous strainburst process. (a) Loading path; (b) failure process. Among them, I_1–I_4 indicate different moment points.

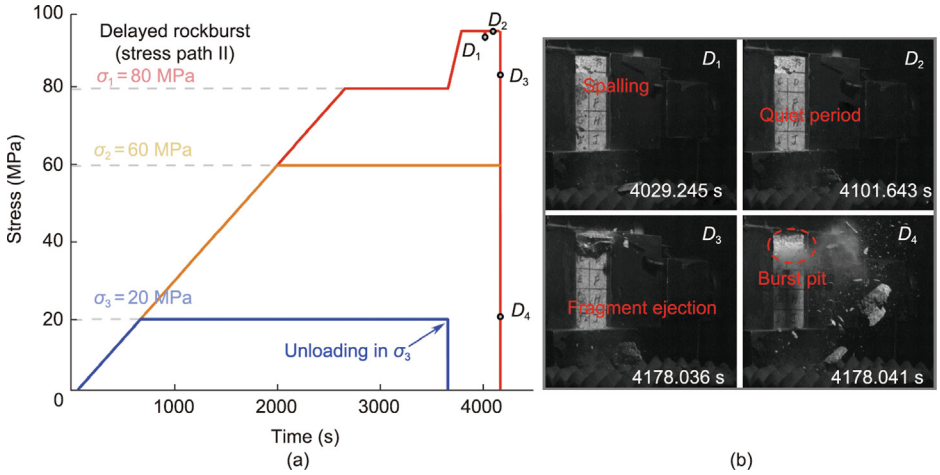

Fig. 3. Delayed strainburst process. (a) Loading path; (b) failure process. Among them, D_1–D_4 indicate different moment points.

restrains the relaxation and deformation of the surrounding rock by supporting at the right time (neither too early nor too late) after excavation. The surrounding rock and supporting structure are monitored to further guide the design and construction of the project. A certain deformation on the surrounding rock is allowed, which recommends "yield before resistance". In essence, it is a low stress compensation support scheme suitable for excavation in middle and shallow strata.

However, in the process of deep underground tunnel excavation, traditional methods find it difficult to adapt to high geostress or to be adopted for the prevention and control of rockburst, severe deformation, and other disasters resulting from surround-

ing rock deformation and failure [1]. Aiming at tackling such a problem, the authors' team [43,44] put forward an active support strategy based on high pre-stress compensation to adapt to deep underground conditions, which is called the ECM. The Mohr stress circle was used to analyze the supporting principle. Fig. 4 exhibits the comparison of the three methods. The green Mohr stress circle represents the initial geo-stress state. Excavation-induced radial stress unloading and tangential stress concentrations are named as excavation effect Ⅰ and excavation effect Ⅱ, respectively, as presented in blue and red in Fig. 4. The black curve is the failure envelope. Affected by the excavation effect, the Mohr stress circle may exceed the failure envelope, leading to surrounding rock instability and even rockburst dynamic failure. By compensating the surrounding rock with high pre-stress support and restoring it to the 3D stress state of the original rock as much as possible, and better utilizing the triaxial strength of the rock instead of uniaxial or biaxial strength, the stability of the surrounding rock will be effectively controlled (the purple Mohr stress circle in Fig. 4). This also avoids the generation of excess energy ΔE, thus reducing the risk of rockburst disaster. The keys to ECM are: sufficiently large pre-stressing to compensate for the reduced radial stresses at the beginning of the excavation, and early support timing to avoid deterioration of the surrounding rock. It recommends "resistance before yield".

2.3. Implementation of the ECM based on the NPR bolt

Traditional bolts, which have low strength and poor toughness, are unable to bear high pre-tightening force applied to them. To overcome this difficulty and realize the ECM, the authors' team [43] developed a new type of bolt made of new steel, called the NPR bolt. New steel boasts exceptional mechanical properties such as high strength, high toughness, impact resistance, and no necking, which are achieved by adding alloying elements and improving the smelting process. This new type of bolt is developed based on the original design concept of the first generation of constant-resistance and large-deformation bolt [45]. The first generation of bolt has achieved constant resistance and large deformation through the design of special structure and has the macroscopic structural effect of an NPR. The new NPR bolt achieves a major innovation at the material level. In order to verify its mechanical properties, static tensile and drop hammer impact tests were carried out on new NPR steel, and the results were compared with that of ordinary Q235 steel.

Fig. 5 depicts the load–displacement curves under static tension. Steel bars with a length of 800 mm and a diameter of 18 mm were used in the test. The yield load of NPR steel is 197.27 kN, 2.21 times that of Q235 steel. The ultimate elongation of NPR steel reaches 33.5%, 1.48 times of that of Q235 steel. Its energy absorption capacity (the area under the curve) is 2.67 times that of Q235 steel. NPR steel exhibits the characteristics close to the ideal elastic–plastic material. In support design, Q235 steel can only use 40%–60% of its tensile strength, while NPR steel can use 90% [43].

The weight of the drop hammer is 1000 kg and the maximum falling height is 1500 mm in the drop hammer impact test. The samples are NPR and Q235 steel bars with a length of 2.8 m and a diameter of 18 mm. The total clamping length of both ends of the sample is 0.3 m, and the effective length is 2.5 m. In the test, the hammer was lifted to the preset height before falling freely and impacting the sample. In order to study the response of the sample under different impact loads, the height of drop hammer increased in turn (10–1200 mm) during the first 17 impacts. Then, the height of 1200 mm was kept unchanged until the sample was destroyed. Fig. 6(a) details the impact force–time curves of NPR and Q235 steel at the tenth impact (falling height is 500 mm) recorded by the sensor at the clamping end. Due to the rebound of the drop hammer, the impact forces of the two materials attenuated in repeated fluctuations. However, NPR steel corresponded to a higher impact force and a longer vibration time. Here, the first waveform, as the main energy absorption process, will be analyzed in detail. The maximum impact force of NPR steel in the tenth impact is 253.1 kN and the first wave duration is 31.9 ms. The maximum impact force of Q235 steel is 190.8 kN and the first wave

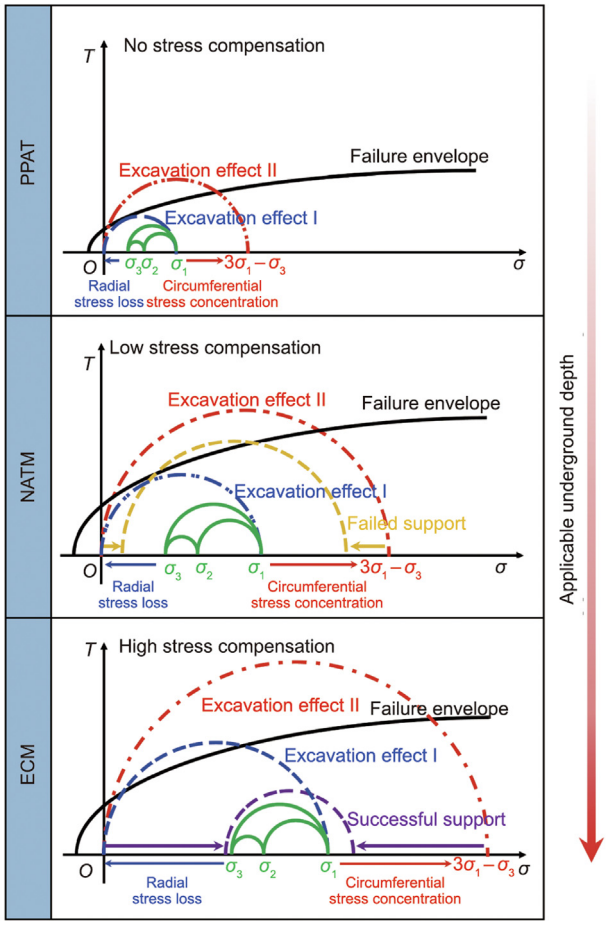

Fig. 4. Principle of the ECM and its comparison with PPAT and NATM. [43].

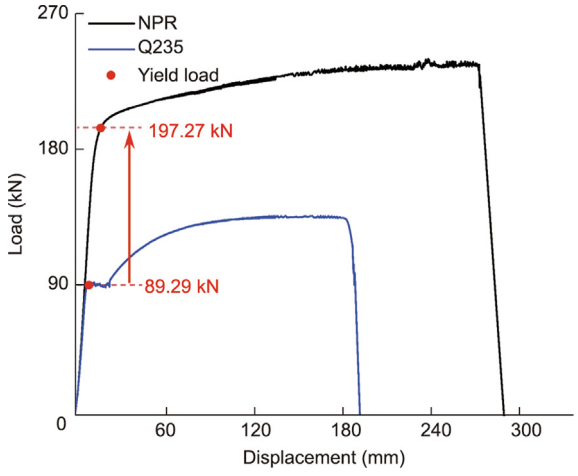

Fig. 5. Load–displacement curves under static tension.

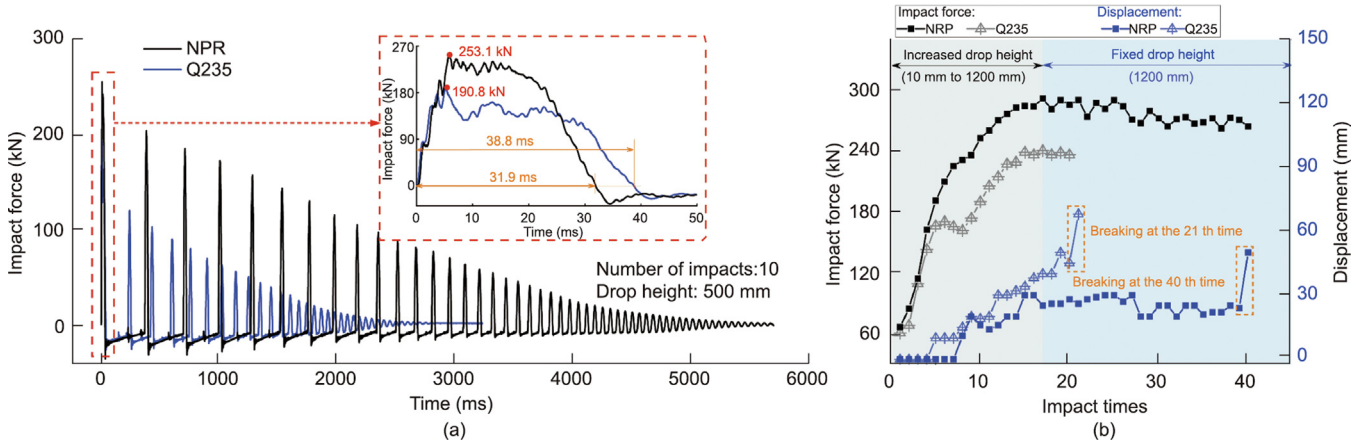

Fig. 6. Drop hammer impact test results. (a) Impact force–time curves of the tenth impact; (b) maximum impact force and final plastic elongation curves.

duration is 38.8 ms. These data suggest that NPR boasts higher dynamic energy absorption efficiency. Fig. 6(b) reveals the maximum impact force and irreversible elongation of the samples at each impact during the whole experiment. The impact force of NPR steel is always higher than that of Q235 steel, and it experiences milder plastic deformation, which reflects its superior dynamic elastic energy absorption. Q235 steel breaks at the 21st impact, while NPR steel endures 40 impacts. Moreover, in both the static test and the dynamic test, the whole bar of NPR steel becomes thinner evenly in the elongation process. Unlike traditional materials, NPR steel does not present partial necking fractures. Fig. 7 indicates typical fractures of NPR steel and Q235 steel.

The extraordinary mechanical properties of NPR bolt make it possible to realize the ECM and control rockburst. The characteristics of high strength and strong toughness are the foundation of remarkable pre-tightening force, and its excellent impact resistance enables it to provide an effective support force under the dynamic load caused by rockburst and external dynamic disturbance, thus ensuring engineering safety.

3. Engineering application of the ECM

3.1. Project overview and geological conditions

The Hanjiang-to-Weihe River Diversion Project is an important south–north water diversion project in Shaanxi Province, China. It aims to solve the water shortage problem in cities along the Weihe River in central Shaanxi area. The water diversion project is mainly composed of the Huangjinxia Water Control Project, the Sanhekou Water Control Project, and the Qinling Water Conveyance Tunnel, which is the key channel of water diversion. Its inlet is located at the control gate of the Sanhekou Water Control Project, and its outlet is Huangchi River in Zhouzhi County. In this study, the test section of the ECM is located in the north section of the Qinling Water Conveyance Tunnel. The length of the TBM excavation with a diameter of 8.02 m in the northern section exceeds 15 km, and the maximum burial depth of the tunnel exceeds 2000 m. The specific bid sections of the test section are pile numbers K43 + 865–K43 + 815, with a length of 50 m and a maximum buried depth of 1837 m. The surrounding rock is relatively complete, its lithology being diorite. Fig. 8 is a schematic diagram of its specific position and adjacent geological profile. The stress in the high buried depth on site is extremely high and is dominated by horizontal tectonic stresses. The maximum horizontal principal stress is estimated to exceed 100 MPa. Instantaneous strainburst disasters occur frequently within a few hours after excavation, and a large number of delayed strainburst events continue to occur for 2–3 days after excavation. Fig. 9(a) indicates the locations and pit depths of 979 rockburst events in the tunnel from January 6, 2020 to January 18, 2022. Most rockburst disasters occurred within the 120° angle of the vault, especially in the direction of 0 o'clock and 1 o'clock. The depth of burst pit is concentrated in the range of > 0.5–1.5 m. Fig. 9(b) shows a typical V-shaped burst pit caused by rockburst at vault of the tunnel, with the maximum depth of 1.1 m.

Fig. 7. Typical fractures of (a) NPR steel (no necking) and (b) Q235 steel (significant necking).

3.2. NPR support design and construction scheme

In the hope of verifying the applicability of the ECM to rockburst disaster control, the field test of high pre-stressed support was carried out on the scheduled test section of the northern section of the Qinling Water Conveyance Tunnel by using the NPR bolt. In the original primary support scheme (Fig. 10(a)), only six ordinary mortar bolts (Φ25 mm × 3500 mm) were applied within 90° of

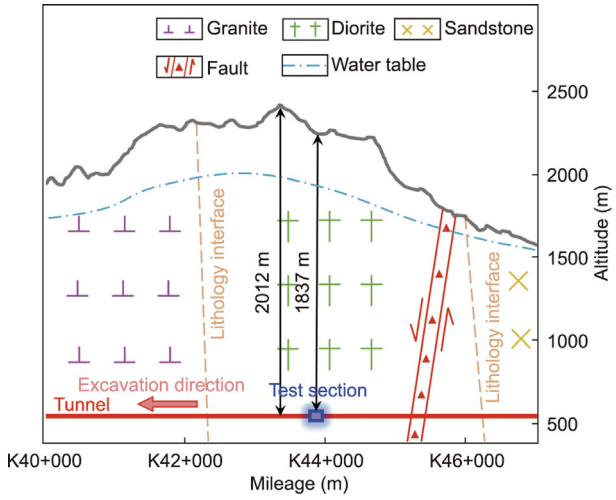

Fig. 8. Geological profile of the test section area.

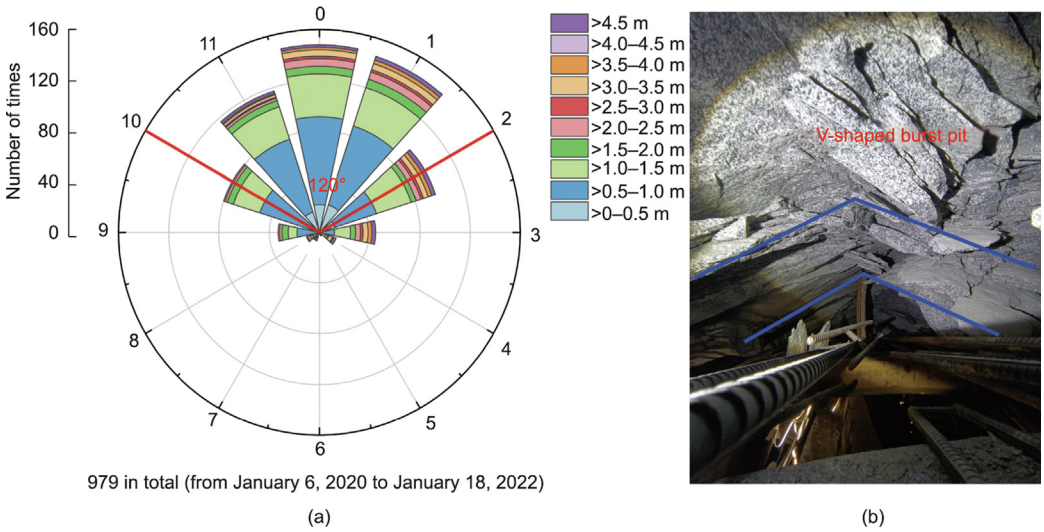

Fig. 9. Situation of rockburst on site. (a) Statistics of burst pit location and depth; (b) a typical V-shaped burst pit on the vault.

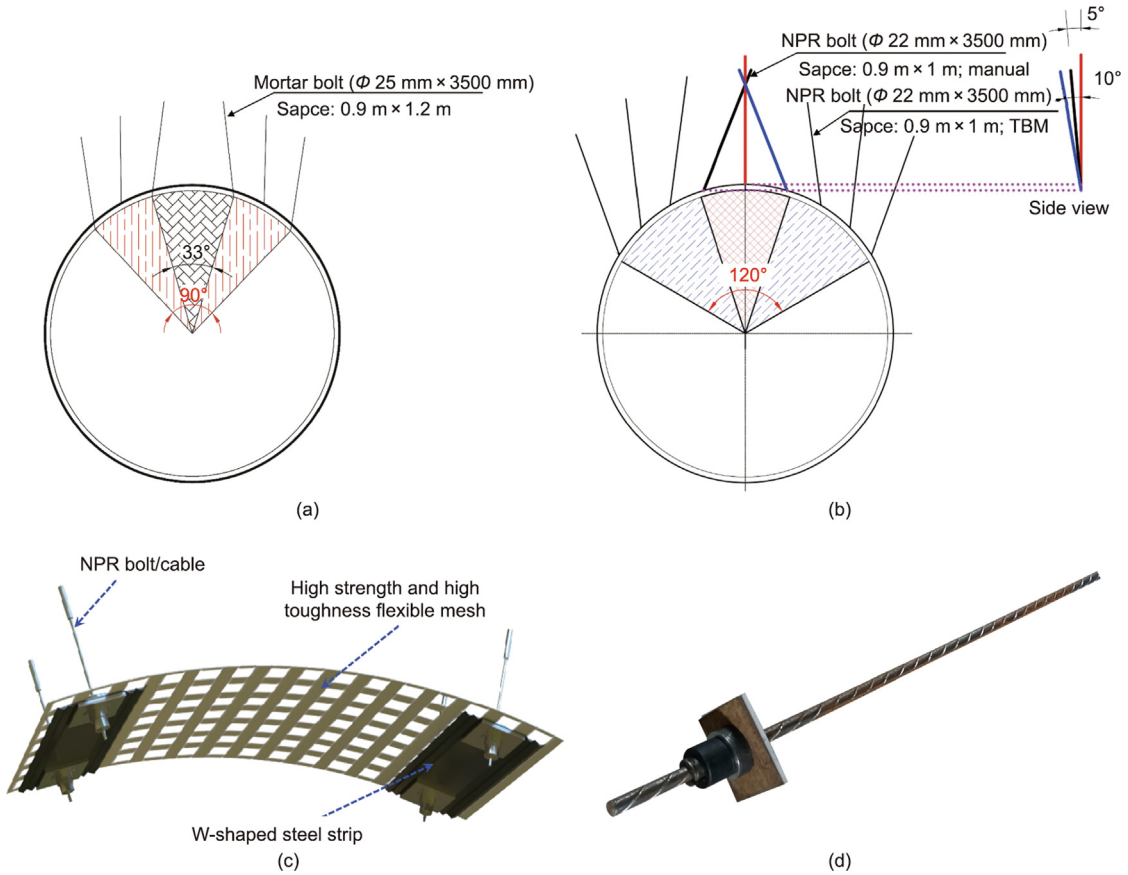

Fig. 10. Improvement of bolt support scheme. (a) Original bolt layout scheme; (b) NPR bolt layout scheme; (c) 3D NPR active support system; (d) NPR bolt used in the field.

the vault and there was no pre-stress. The row spacing of bolts was 1.2 m. Around 30° of the vault was left unprotected, where rockburst was highly possible to occur. Moreover, H150 steel arch frame and longitudinal steel bar row were applied for support. The spacing of steel arches was 0.9 m. After the steel arch was closed, C20 concrete was poured inside. The support scheme shown in Fig. 10(b) mainly improved the layout of the bolts. Nine NPR bolts (Φ22 mm × 3500 mm) were arranged in the main rockburst area (120° of the vault). The row spacing of bolts was 1 m. In order to strengthen the support within 30° of the vault, three NPR bolts were set. To prevent crossing, the three bolts had a deflection angle of 5° on the side. In addition, a 3D NPR active support system, which was composed of NPR bolt, W-shaped steel belt, and high-strength and high-toughness flexible mesh, was designed and installed in the field. The NPR bolt provided the supporting force; the W-shaped steel belt played a fixing and connecting role; and

the flexible mesh played a protective role by preventing rock fragments from flying out. Figs. 10(c) and (d) present the schematic diagram of the 3D NPR active support system and the physical diagram of the NPR bolt used in the field, respectively. During the construction, six NPR bolts were drilled by the TBM. Three of them in the vaults need to be drilled manually because of the existence of blind spots in the TBM. After the bolt was installed, a 200 kN pretightening force was quickly applied to it within 30 min. The whole construction process required timely active support and rapid pretightening to realize high pre-stress compensation.

Traditional TBMs adopt passive support and have a large blind area, making it difficult to meet the requirements of the ECM. Therefore, State Key Laboratory for Geomechanics and Deep Underground Engineering (Beijing, China) recently designed and developed a new tunneling equipment called the Rockburst-NPR TBM. In contrast, the Rockburst-NPR TBM is designed based on the active support concept of the ECM. It can realize the rapid construction of 3D NPR active support system in the range of 280° during excavation. Besides, it is equipped with an expanding cutterhead, a cascade shield system (including first level shield and secondary radial retractable shield), an anchor–hole drilling system with nine sets in three districts, a flexible mesh laying system, an advanced treatment (advanced detection, advanced grouting, and advanced reinforcement) system with seven set points, and a preliminary concrete spraying system. Fig. 11 presents its design sketch. It is believed that the Rockburst-NPR TBM will provide powerful equipment support for rockburst control in TBM excavation of deep underground engineering in the future.

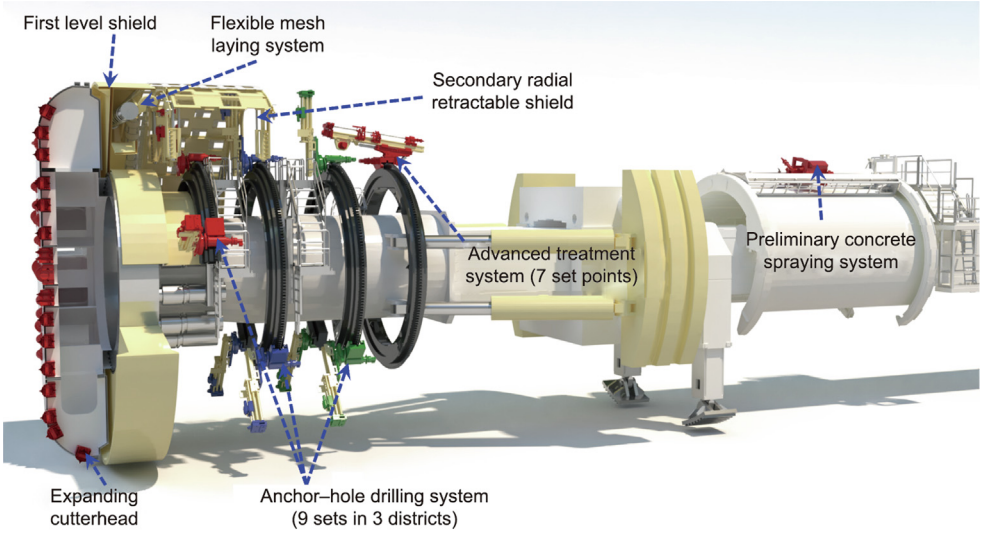

Fig. 11. Design sketch of Rockburst-NPR TBM.

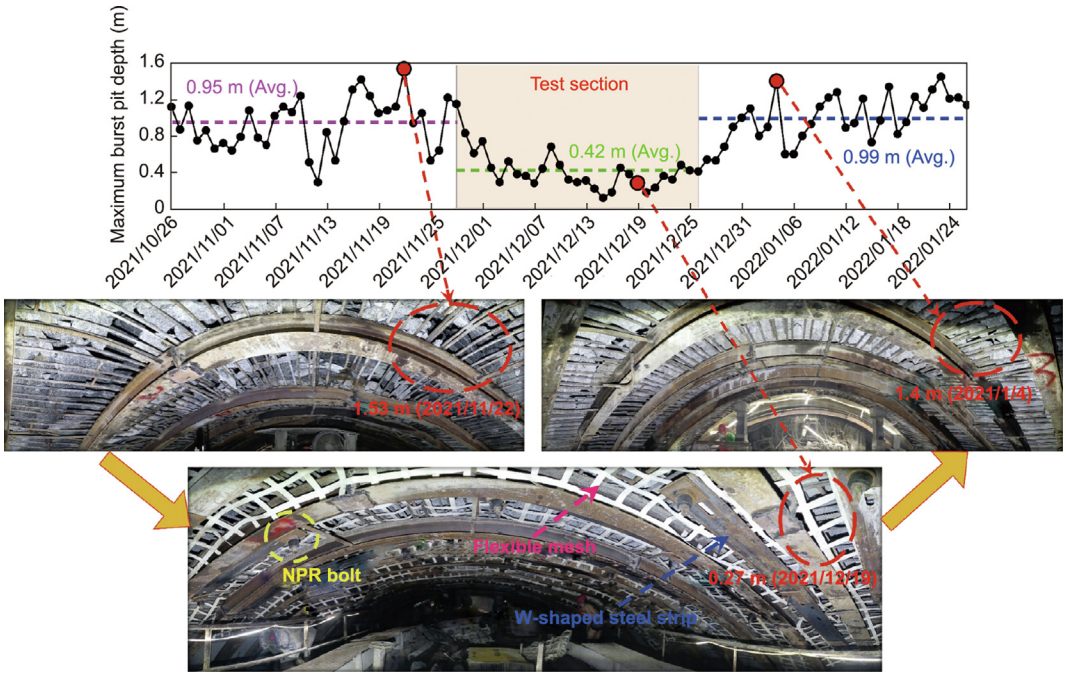

Fig. 12. Maximum depth of burst pit during excavation and on-site rockburst situation. Avg.: average.

3.3. Rockburst control effect

After the construction of the test section according to the improved support scheme, the rockburst disaster has been significantly controlled. Fig. 12 counts the deepest burst pit depth at the corresponding tunneling position and the specific damage situation at individual positions during the construction period from October 26, 2021 to January 27, 2022. In the position before the test section, the average depth of burst pit reached 0.95 m. During the tunneling process of the test section (from November 28, 2021 to December 26, 2021), the average depth of burst pit was 0.42 m. The result fully demonstrates that the implementation of the ECM greatly relieved the rockburst damage on site. At the position behind the test section, the rockburst returned to a severe level, and the average depth of the burst pit was 0.99 m. The force on the support structure and the deformation of the surrounding rock at different positions were monitored. Fig. 13(a) indicates the stress of bolt and steel arch at the vault positions of several typical sections in the test section after tunnel deformation convergence. The red and green lines indicate the bolt and steel arch forces, respectively. Positive values mean being in tension and negative values mean being in compression. In addition, for comparison, the typical sections (pile numbers K43 + 875 and K43 + 805) without NPR bolt support in front of and behind the test section are also displayed. Fig. 13(b) shows the deformation of surrounding rock at different positions. Negative values in the figure represent that the reserved deformation (200 mm) is not exceeded, while positive values represent the opposite. Under the active support of high pre-stressed NPR bolts, the deformation of surrounding rock was effectively controlled, and the stress of steel arch was significantly reduced. For example, the average pressures on the vault of steel arch at K43 + 875 and K43 + 805 were about 49 and 44.4 MPa,

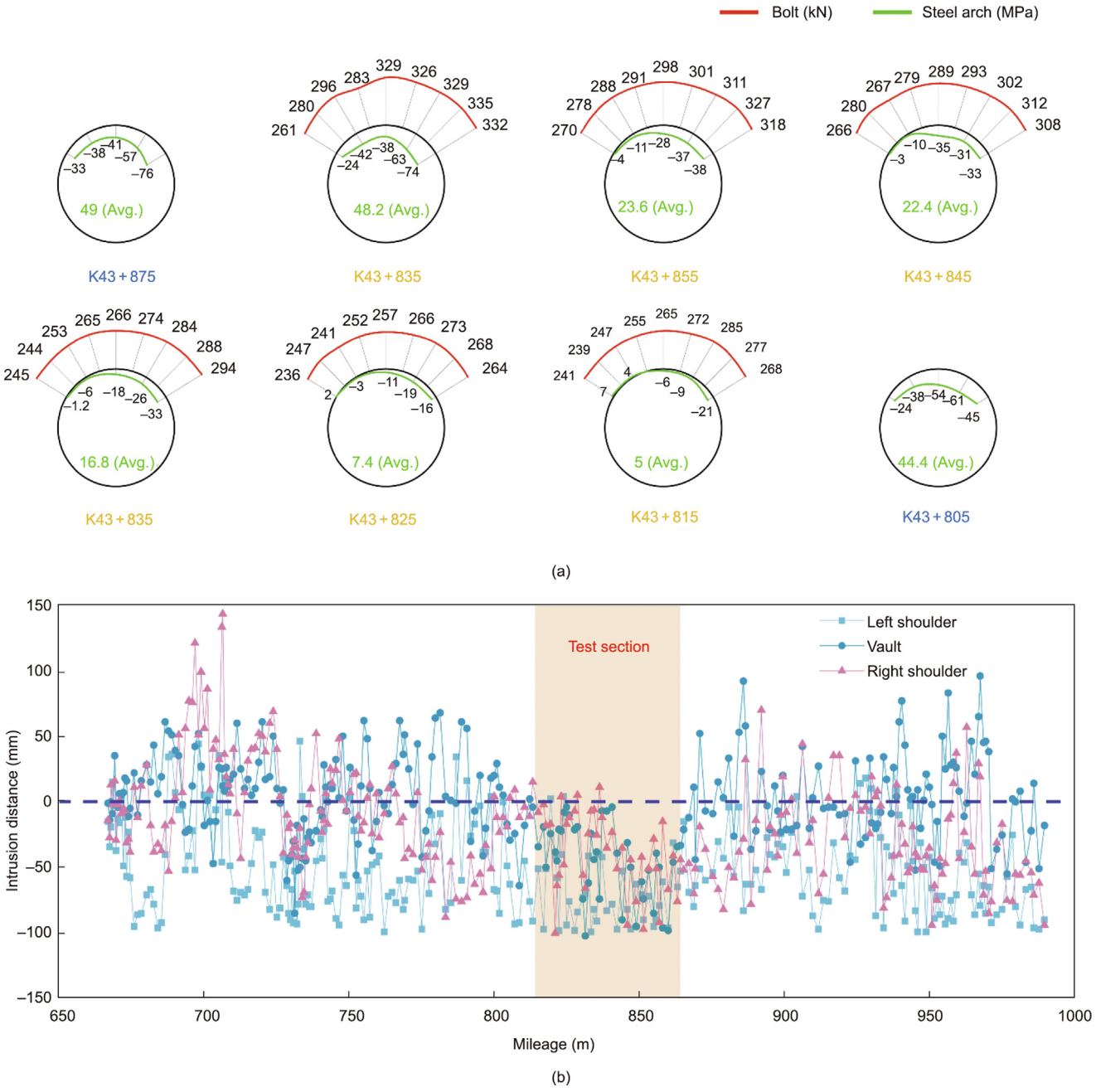

Fig. 13. (a) Pressure on steel arches and bolts at different positions; (b) intrusion distance of the surrounding rock.

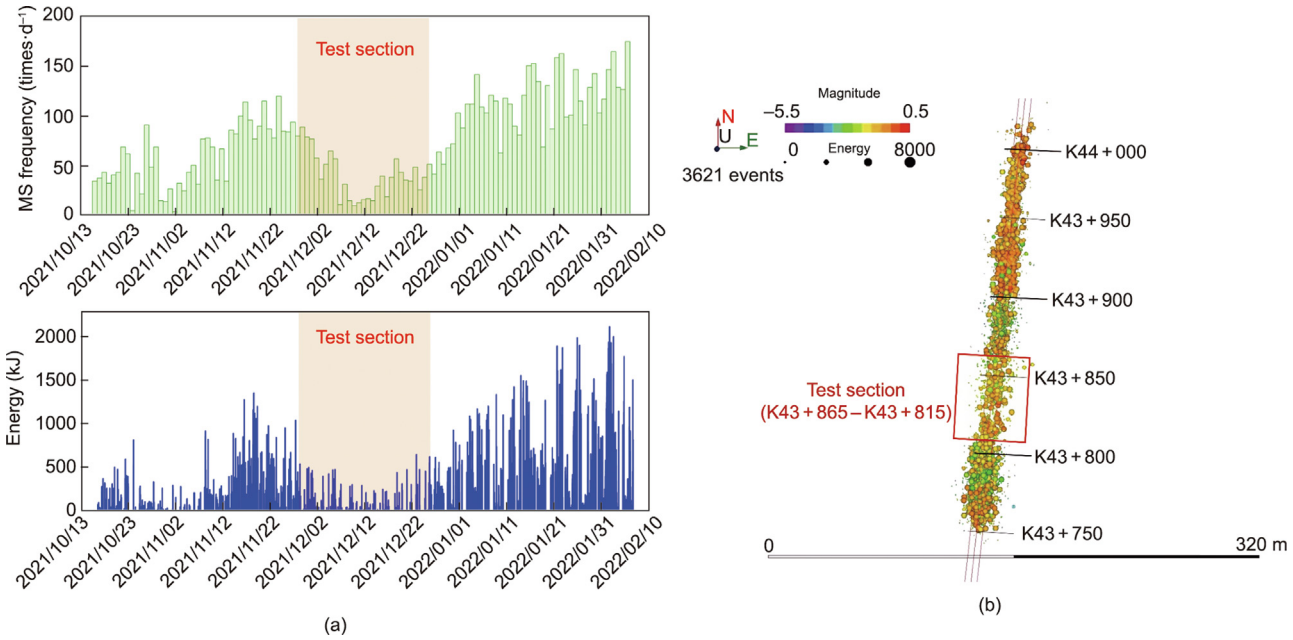

Fig. 14. Microseismic monitoring results. (a) Frequency and energy; (b) 3D positioning.

respectively, while the pressure in the test section was generally less than this stress level. In the test section, the deformation of surrounding rock ranged from −100 mm to 0 mm, basically not exceeding the reserved deformation.

Microseism (MS) is a remote, 3D, and continuous rock mass fracture monitoring technology that can capture elastic waves released during rockburst [46]. As the time, location, intensity, and even fracture mechanism of rockburst can be obtained by wave analysis, MS has been widely used for rockburst monitoring and early warning. The high-resolution MS monitoring system manufactured by Engineering Seismology Group (ESG, Canada), was applied to rockburst monitoring in this project. For specific information, please refer to Wang et al. [47]. MS events during tunneling from October 13, 2010 to February 10, 2022 were continuously monitored, and the results are illustrated in Fig. 14. During the tunneling period of the test section (November 28, 2021 to December 26, 2021), the frequency and energy value of MS signals decreased notably. The frequency was below 65 times·d^{-1}, and the energy was lower than 500 kJ. The 3D positioning map also shows the low density and small magnitude of MS events in the test section, reflecting that ECM weakened rockburst damage.

4. Conclusion and summary

This study is aimed at the difficult problems of rockburst disaster control in deep underground excavation. First, the mechanism of rockburst and the supporting principle of the ECM suitable for high ground stress conditions were briefly summarized, and it was proposed to apply the ECM to rockburst control. Moreover, the field test was carried out in the Qinling Water Conveyance Tunnel of the Hanjiang–Weihe River Water Diversion Project. Specifically, excavation will lead to radial stress unloading and tangential stress concentration of the surrounding rock, and the excess energy ΔE generated by the change in the engineering stress state is the fundamental cause of rockburst. The true triaxial loading and single-side unloading test carried out in laboratory confirmed this point. The ECM is an active support strategy, which counteracts the excavation effect by high pre-stress compensation and reduces the risk of rockburst. The new NPR bolt developed serves as the material foundation of the ECM. The results of static and dynamic mechanical tests reveal that it has the constant mechanical characteristics of high strength, high toughness, impact resistance, and no necking, and can realize a high pre-tightening force and resist the impact of rockburst (and dynamic disturbance). Finally, the field test demonstrates that the 3D NPR active support system can effectively control the rockburst disaster. This point is verified by the depth of burst pit, the stress of supporting equipment, the deformation of surrounding rock, and the results of microseismic monitoring. Therefore, the research fully proves that the ECM is scientific and effective in controlling rockburst.

Acknowledgments

This research was supported by the National Natural Science Foundation of China (41941018), the Foundation of State Key Laboratory for Geomechanics and Deep Underground Engineering (SKLGDUEK 2217), and the Foundation of Collaborative Innovation Center for Prevention and Control of Mountain Geological Hazards of Zhejiang Province (PCMGH-2022-03). In addition, we acknowledge the support of Prof. Chunan Tang from Dalian University of Technology and Dr. Yucheng Wang from Northeastern University in Microseismic monitoring.

Compliance with ethics guidelines

Jie Hu, Manchao He, Hongru Li, Zhigang Tao, Dongqiao Liu, Tai Cheng, and Di Peng declare that they have no conflict of interest or financial conflicts to disclose.

References

[1] He M, Cheng T, Qiao Y, Li H. A review of rockburst: experiments, theories, and simulations. J Rock Mech Geotech Eng 2023;15(5):1312–53.
[2] Feng GL, Feng XT, Chen B, Xiao YJ, Yu Y. A microseismic method for dynamic warning of rockburst development processes in tunnels. Rock Mech Rock Eng 2015;48(5):2061–76.
[3] Xu ZX, Zhang LG, Jiang LW, Wang K, Zhang GZ, Feng T, et al. Engineering geological environment and main engineering geological problems of Ya'an–Linzhi section of the Sichuan–Tibet Railway. Adv Eng Sci 2021;53(3):29–42. Chinese.

[4] Cook NGW. The basic mechanics of rockbursts. J South Afr Inst Min Metall 1963;64(3):71–81.
[5] Ortlepp WD, Stacey TR. Rockburst mechanisms in tunnels and shafts. Tunnelling Underground Space Technol 1994;9(1):59–65.
[6] Su G, Hu L, Feng X, Yan L, Zhang G, Yan S, et al. True triaxial experimental study of rockbursts induced by ramp and cyclic dynamic disturbances. Rock Mech Rock Eng 2018;51(4):1027–45.
[7] Akdag S, Karakus M, Nguyen GD, Taheri A, Bruning T. Evaluation of the propensity of strain burst in brittle granite based on post-peak energy analysis. Underground Space 2021;6(1):1–11.
[8] Akdag S, Karakus M, Nguyen GD, Taheri A. Strain burst vulnerability criterion based on energy-release rate. Eng Fract Mech 2020;237:107232.
[9] Keneti A, Sainsbury BA. Review of published rockburst events and their contributing factors. Eng Geol 2018;246:361–73.
[10] Li T, Ma C, Zhu M, Meng L, Chen G. Geomechanical types and mechanical analyses of rockbursts. Eng Geol 2017;222:72–83.
[11] Cheng T, He M, Li H, Liu D, Qiao Y, Hu J. Experimental investigation on the influence of a single structural plane on rockburst. Tunnelling Underground Space Technol 2023;132:104914.
[12] Akdag S, Karakus M, Taheri A, Nguyen G, He M. Effects of thermal damage on strain burst mechanism for brittle rocks under true-triaxial loading conditions. Rock Mech Rock Eng 2018;51(6):1657–82.
[13] He M, Xia H, Jia X, Gong W, Zhao F, Liang K. Studies on classification, criteria and control of rockbursts. J Rock Mech Geotech Eng 2012;4(2):97–114.
[14] Singh SP. Burst energy release index. Rock Mech Rock Eng 1988;21(2):149–55.
[15] Wawersik WR, Fairhurst C. A study of brittle rock fracture in laboratory compression experiments. Int J Rock Mech Min Sci 1970;7(5):561–75.
[16] Luo S, Gong F, Peng K, Liu Z. Influence of water on rockburst proneness of sandstone: insights from relative and absolute energy storage. Eng Geol 2023;323:107172.
[17] Li H, He M, Qiao Y, Cheng T, Xiao Y, Gu Z. Mode I fracture properties and energy partitioning of sandstone under coupled static–dynamic loading: implications for rockburst. Theor Appl Fract Mech 2023;127:104025.
[18] Li H, Qiao Y, He M, Shen R, Gu Z, Cheng T, et al. Effect of water saturation on dynamic behavior of sandstone after wetting–drying cycles. Eng Geol 2023;319:107105.
[19] He MC, Miao JL, Feng JL. Rock burst process of limestone and its acoustic emission characteristics under true-triaxial unloading conditions. Int J Rock Mech Min Sci 2010;47(2):286–98.
[20] Zhou J, Li X, Mitri HS. Evaluation method of rockburst: state-of-the-art literature review. Tunnelling Underground Space Technol 2018;81:632–59.
[21] Sepehri M, Apel DB, Adeeb S, Leveille P, Hall RA. Evaluation of mining-induced energy and rockburst prediction at a diamond mine in Canada using a full 3D elastoplastic finite element model. Eng Geol 2020;266:105457.
[22] Feng XT, Liu J, Chen B, Xiao Y, Feng G, Zhang F. Monitoring, warning, and control of rockburst in deep metal mines. Engineering 2017;3(4):538–45.
[23] Li H, Qiao Y, Shen R, He M, Cheng T, Xiao Y, et al. Effect of water on mechanical behavior and acoustic emission response of sandstone during loading process: phenomenon and mechanism. Eng Geol 2021;294:106386.
[24] Dong L, Hu Q, Tong X, Liu Y. Velocity-free MS/AE source location method for three-dimensional hole-containing structures. Engineering 2020;6(7):827–34.
[25] Dong L, Zou W, Li X, Shu W, Wang Z. Collaborative localization method using analytical and iterative solutions for microseismic/acoustic emission sources in the rockmass structure for underground mining. Eng Fract Mech 2019;210:95–112.
[26] Qiu L, Liu Z, Wang E, He X, Feng J, Li B. Early-warning of rock burst in coal mine by low-frequency electromagnetic radiation. Eng Geol 2020;279:105755.
[27] Cao K, Dong F, Yu Y, Khan NM, Hussain S, Alarifi SS. Infrared radiation response mechanism of sandstone during loading and fracture process. Theor Appl Fract Mech 2023;126:103974.
[28] Cai W, Dou L, Si G, Hu Y. Fault-induced coal burst mechanism under mining-induced static and dynamic stresses. Engineering 2021;7(5):687–700.
[29] Pu Y, Apel DB, Wei C. Applying machine learning approaches to evaluating rockburst liability: a comparation of generative and discriminative models. Pure Appl Geophys 2019;176(10):4503–17.
[30] He M, e Sousa LR, Miranda T, Zhu G. Rockburst laboratory tests database—application of data mining techniques. Eng Geol 2015;185:116–30.
[31] Konicek P, Soucek K, Stas L, Singh R. Long-hole destress blasting for rockburst control during deep underground coal mining. Int J Rock Mech Min Sci 2013;61:141–53.
[32] Gong F, He Z, Si X. Experimental study on revealing the mechanism of rockburst prevention by drilling pressure relief: status-of-the-art and prospects. Geomatics Nat Hazards Risk 2022;13(1):2442–70.
[33] Huang B, Liu C, Fu J, Guan H. Hydraulic fracturing after water pressure control blasting for increased fracturing. Int J Rock Mech Min Sci 2011;48(6):976–83.
[34] Kaiser PK, Cai M. Design of rock support system under rockburst condition. J Rock Mech Geotech Eng 2012;4(3):215–27.
[35] Cai M. Principles of rock support in burst-prone ground. Tunnelling Underground Space Technol 2013;36:46–56.
[36] Charette F, Plouffe M. Roofex®—results of laboratory testing of a new concept of yieldable tendon. In: Potvin Y, editor. Deep mining 2007: proceedings of the fourth international seminar on deep and high stress mining; 2007 Nov 7–9; Perth, WA, Australia. Perth: Australian Centre for Geomechanics; 2007. p. 395–404.
[37] Varden R, Lachenicht R, Player JR, Thompson A, Villaescusa E. Development and implementation of the Garford dynamic bolt at the Kanowna Belle Mine. In: 10th underground operators' conference; 2008 Apr 14–16; Launceston, TAS, Australia. Launceston: the Australasian Institute of Mining and Metallurgy; 2008. p. 95–104.
[38] Li CC. A new energy-absorbing bolt for rock support in high stress rock masses. Int J Rock Mech Min Sci 2010;47(3):396–404.
[39] Wu YK, Oldsen J. Development of a new yielding rock bolt—Yield-Lok bolt. In: the 44th US Rock Mechanics Symposium and 5th US–Canada Rock Mechanics Symposium; 2010 Jun 27–30; Salt Lake City, UT, USA. Alexandria: the American Rock Mechanics Association; 2010. p. ARMA-10-197.
[40] He M, Li J, Liu D, Ling K, Ren F. A novel true triaxial apparatus for simulating strain bursts under high stress. Rock Mech Rock Eng 2021;54:759–75.
[41] Fan H, Li L, Liu H, Hu J, Zhang M, Zhou S, et al. Improvement to the calculating model of the pressure arch's height considering the confining pressure in the excavation of shallow tunnels. Arabian J Geosci 2021;14(12):1130.
[42] Rabcewicz LV. The new Austrian tunnelling method. Water Power 1964;17:453–7.
[43] He M, Sui Q, Li M, Wang Z, Tao Z. Compensation excavation method control for large deformation disaster of mountain soft rock tunnel. Int J Min Sci Technol 2022;32(5):951–63.
[44] He M, Wang Q. Excavation compensation method and key technology for surrounding rock control. Eng Geol 2022;307:106784.
[45] He M, Gong W, Wang J, Qi P, Tao Z, Du S, et al. Development of a novel energy-absorbing bolt with extraordinarily large elongation and constant resistance. Int J Rock Mech Min Sci 2014;67:29–42.
[46] Liu F, Tang C, Ma T, Tang L. Characterizing rockbursts along a structural plane in a tunnel of the Hanjiang-to-Weihe river diversion project by microseismic monitoring. Rock Mech Rock Eng 2019;52:1835–56.
[47] Wang Y, Tang CA, Tang L, Zhang S, Li L, Li Y, et al. Microseismicity characteristics before and after a rockburst and mechanisms of intermittent rockbursts in a water diversion tunnel. Rock Mech Rock Eng 2021;55(1):341–61.
[48] Wang X, Wang E, Liu X, Zhou X. Micromechanisms of coal fracture: Insights from quantitative AE technique. Theor Appl Fract Mech 2021;114:103000.